Single-Event Effects Test Report of the HVD233-SP CAN Bus Transceivers

Joel Cruz-Colon, Veeraraghavan Narayanan, Wade Vonbergen, and Dr. Robert Baumann

ABSTRACT

This study characterized the effect of heavy-ion irradiation on the single-event effect (SEE) performance of the *HVD233-SP CAN Transceiver*. Heavy-ions with LET_{EFF} of 20.12 to 92.01 MeV-cm^2/mg were used to irradiate three production devices in 32 runs with a fluence from 1.0×10^6 to 1.0×10^7 ions/cm^2. The results demonstrate that the HVD233-SP is SEL-free up to $LET_{EFF} = 92.01$ MeV-cm^2/mg at 125°C, and a dynamic SET cross section is presented.

For questions or comments please contact hirelmarketing@list.ti.com.

Contents

List of Figures

List of Tables

Trademarks

DuPont is a trademark of E.I. du Pont de Nemours and Company.
Kevlar is a registered trademark of E.I. du Pont de Nemours and Company.
LabVIEW is a trademark of National Instruments Corporation.
All other trademarks are the property of their respective owners.

1 Overview

The HVD233-SP is a radiation-hardened CAN Bus Transceiver for use in accordance with the ISO 11898 standard. The HVD233-SP can be used to transmit and receive data between a CAN controller and a CAN bus up to 1 Mbps. The device features cross-wire protection, overvoltage protection up to ±16 V, loss-of-ground protection, overtemperature (thermal shutdown) protection, and a common-mode transient of ±100 V. The HVD233-SP can operate over a wide –7-V to 12-V common-mode range.

For more information on the HVD233-SP device, see http://www.ti.com/product/SN55HVD233-SP/technicaldocuments.

Table 1. Overview Information[1]

TI Part Number	HVD233-SP
SMD Number	5962L1420901VX
Device Function	CAN Bus Transceiver
Technology	LBC3S
Exposure Facility	Radiation Effects Facility, Cyclotron Institute, Texas A&M University
Heavy Ion Fluence per Run	$1.0 \times 10^6 - 1.0 \times 10^7$ ions/cm^2
Irradiation Temperature	25°C and 125°C (for SEL testing)

[1] TI may provide technical, applications or design advice, quality characterization, and reliability data or service providing these items shall not expand or otherwise affect TI's warranties as set forth in the Texas Instruments Incorporated Standard Terms and Conditions of Sale for Semiconductor Products and no obligation or liability shall arise from Semiconductor Products and no obligation or liability shall arise from TI's provision of such items.

2 SEE Mechanisms

The primary single-event effect (SEE) events of interest in the HVD233-SP are single-event latch-up (SEL), single-event burn-out (SEB), and single-event transient (SET). From a risk or impact point-of-view, the occurrence of an SEL and SEB is potentially the most destructive SEE event and the biggest concern for space applications. In mixed technologies such as the LBC3S process used for the HVD233-SP, the CMOS circuitry introduces a potential for SEL and SEB susceptibility. SEL can occur if excess current

injection caused by the passage of an energetic ion is high enough to trigger the formation of a parasitic cross-coupled PNP and NPN bipolar structure (formed between the p-sub and n-well and n+ and p+ contacts).[1][2] The parasitic bipolar structure initiated by a single-event creates a high-conductance path (inducing a steady-state current that is typically orders-of-magnitude higher than the normal operating current) between power and ground that persists (is *latched*) until power is removed or until the device is destroyed by the high-current state. The process modifications applied for SEL-mitigation were sufficient as the HVD233-SP exhibited no SEL with heavy-ions up to an LET_{EFF} of 92.01 MeV-cm^2/mg at a fluence of 1.0 × 10^7 ions/cm^2 and a chip temperature of 125°C.

The block diagram in Figure 1 infers that a SET can be induced on the HVD233-SP from primarily two functional blocks. SETs can be introduced from the input-driver circuits to the bus-driver circuit, and the bus-receiver path to the single-ended receiver output. A heavy ion strike affecting the driver input or bus driver will be observed on the Bus CANH, CANL pins, and receiver output R. Otherwise, events on the bus receiver path to the receiver output R will be observed only on the receiver and not the bus. In this report, events are classified as the following:

1. Driver events
2. Receiver events
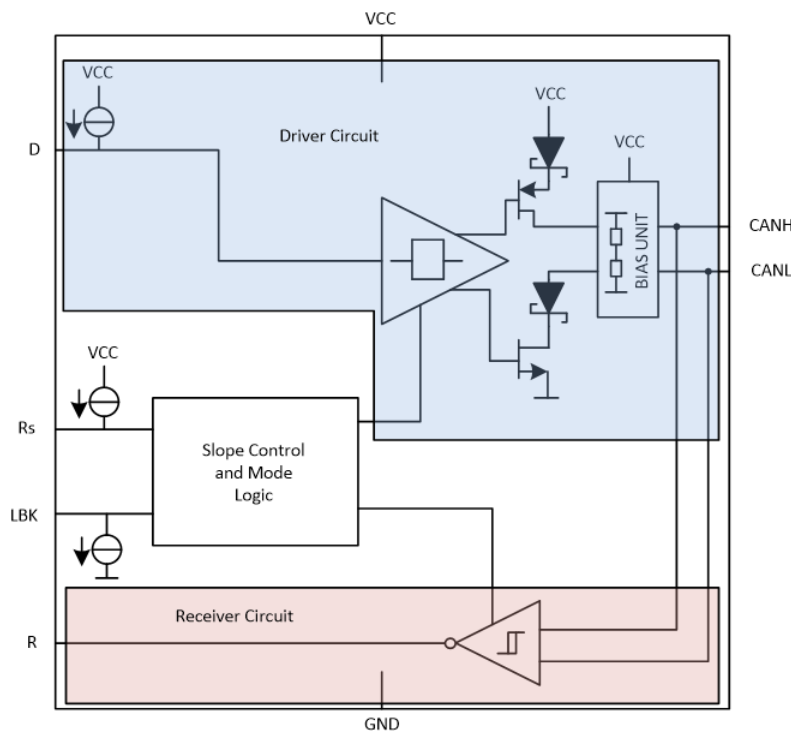
Figure 1. Functional Block Diagram of the HVD233-SP CAN Bus Transceiver

3 Test Device and Test Board Information

The HVD233-SP is packaged in an 8-pin thermally-enhanced dual ceramic flat-pack package (CFP) shown with the pinout in Figure 2. The CDCLVP111 evaluation board used for the SEE characterization is shown in Figure 3.
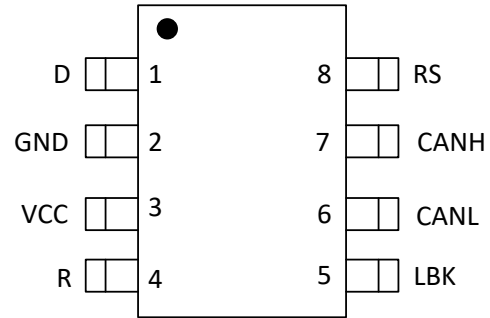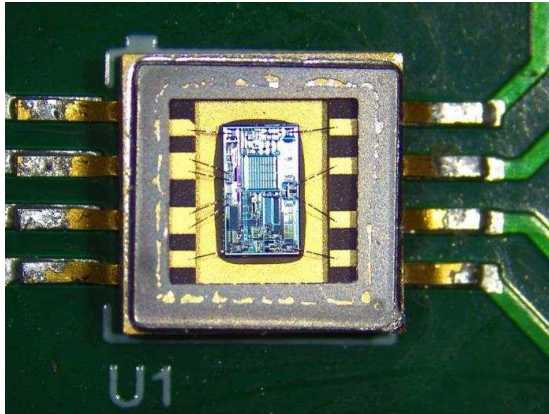
The package lid was removed to reveal the die face for all heavy ion testing.

Figure 2. HVD233-SP Photograph (Left) and a Pinout Diagram (Right)
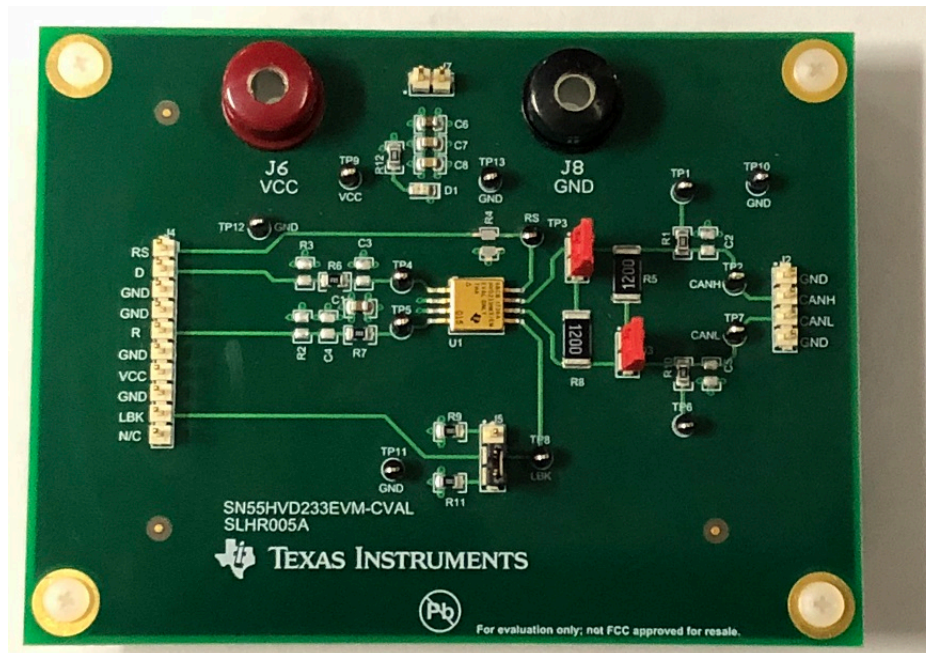
Figure 3. HVD233-SP Mounted on SN55HVD233EVM-CVAL

A schematic of the SN55HVD233EVM-CVAL is illustrated in Figure 4.
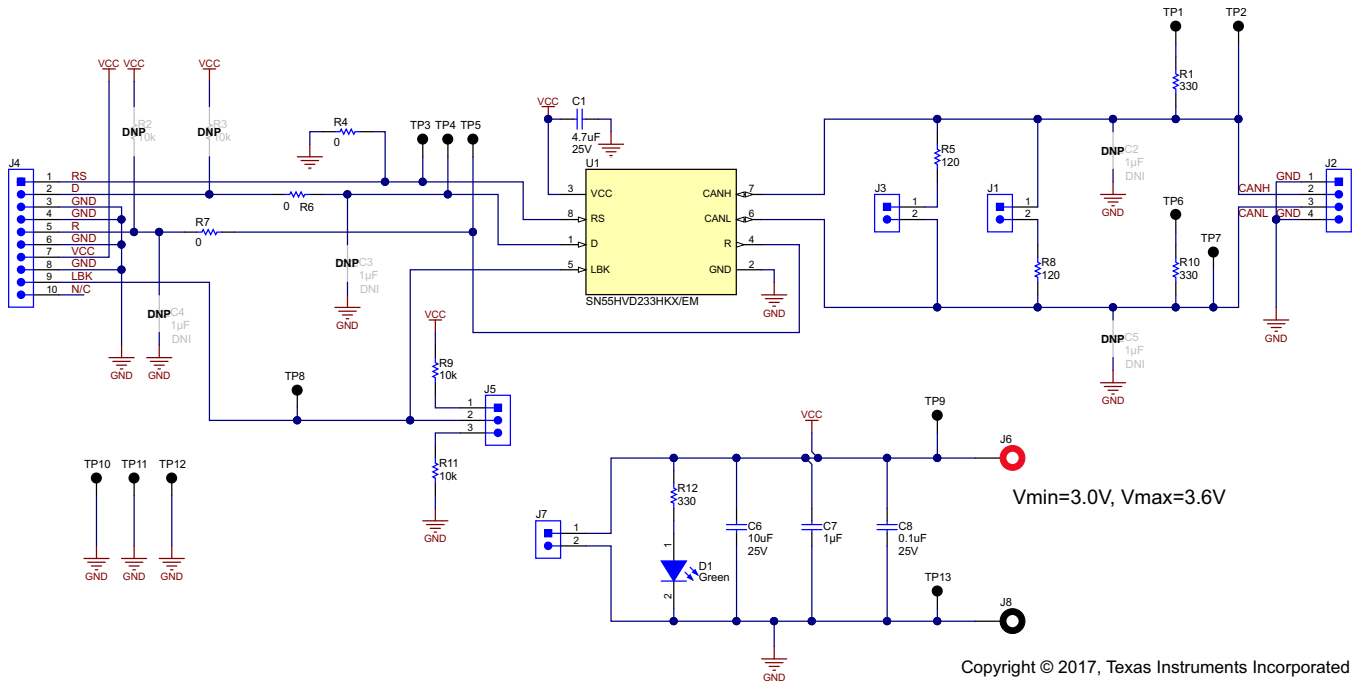
Figure 4. SN55HVD233EVM-CVAL Schematic Evaluation Board Used to Perform the SEE

4   Irradiation Facility and Setup

The heavy ion species used for the SEE studies on this product were provided and delivered by the *TAMU Cyclotron Radiation Effects Facility*[3] using a superconducting cyclotron and advanced electron cyclotron resonance (ECR) ion source. Ion beams are delivered with high uniformity over a 1" diameter circular cross-sectional area for the in-air station. Uniformity is achieved by means of magnetic defocusing. The intensity of the beam is regulated over a broad range spanning several orders of magnitude. For the bulk of these studies, ion fluxes between 1.0×10^4 and 1.0×10^5 ions/sec-cm^2 were used to provide heavy ion fluences between 1.0×10^6 and 1.0×10^7 ions/cm^2. For these experiments, Copper (Cu), Krypton (Kr), and Praseodymium (Pr) ions were used. Ion beam uniformity for all tests was in the range of 91% to 98%. The SN55HVD233EVM-CVAL test board is shown in Figure 5 as it was used at the TAMU facility. The 1-mil Aramica (DuPont™ Kevlar®) window allows in-air testing while maintaining the vacuum within the accelerator with only minor ion energy loss. The air space between the device and the ion beam port window was maintained at 40 mm for all runs. For more information on the effective LET, range and depth for the experiments, please refer to Table 2. For information on the test conditions for each run, see Table 4 and Table 5.
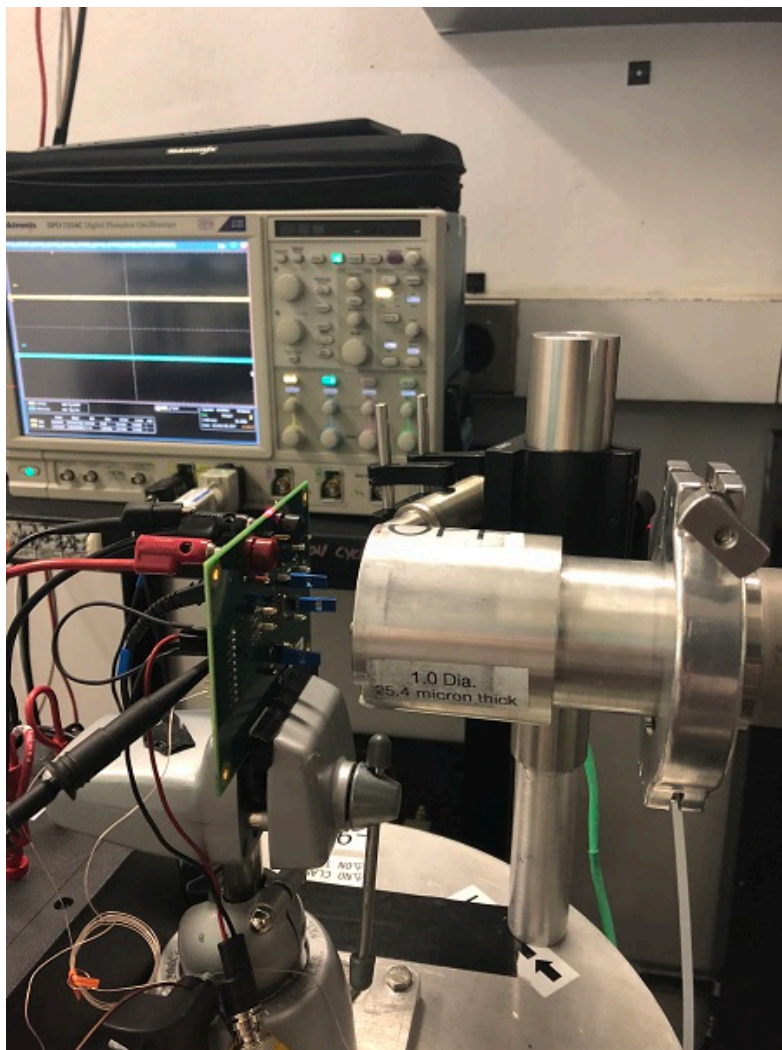
Taken at the TAMU accelerator facility with a 40-mm air gap.

Figure 5. SN55HVD233EVM-CVAL Evaluation Board Mounted in Front of the Heavy Ion Beam Exit Port

5   Depth, Range, and LET$_{EFF}$ Calculation

The HVD233-SP is fabricated in the Texas Instruments Linear LBC3S process with a back-end-of-line (BEOL) stack consisting of two levels of standard thickness aluminum metal. Since LET for any given ion is largely a function of the density of the material through which the ion is traveling, and since the density of aluminum (2.70 g/cm^3) and silicon oxide (2.65 g/cm^3) are similar, the stack is modeled as a homogeneous layer of silicon dioxide. The thickness from the surface of the passivation to the silicon surface is 5020 nm, based on nominal layer thickness as shown in Figure 6.

The left side of the image in Figure 6 shows a generalized LBC3S technology BEOL stack on the HVD233-SP cross section. The right side of the image shows the GUI of RADsim-IONS application used to determine key ion parameters: LET$_{EFF}$, depth, and range for a given ion type, energy, and stack.
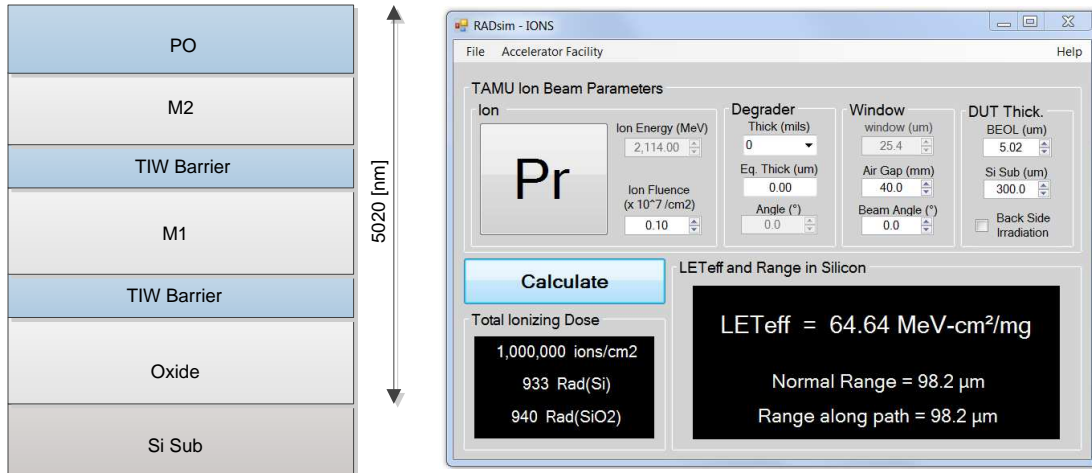
Figure 6. LBC3S Technology BEOL Stack on the HVD233-SP Cross Section (Left) - RADsim-IONS Application GUI (Right)

Accounting for energy loss through the 1-mil thick Aramica (DuPont™ Kevlar®) beam port window, the 40-mm air gap, and the BEOL stack over the HVD233-SP, the effective LET (LET$_{EFF}$) at the surface of the silicon substrate and the depth and ion range was determined with the custom RADsim-IONS application (custom tool developed at Texas Instruments and based on SRIM[4] simulations) for the three ions used for the experiments. For the results, see Table 2.

Table 2. Ion Used for SEE Characterization LET$_{EFF}$, Depth, and Range in Silicon

Ion Type	Angle of Incidence	Depth in Silicon (µm)	Range in Silicon (µm)	LET$_{EFF}$ (MeV-cm^2/mg)
Cu	0	118.4	118.4	20.12
Kr	0	112	112	30.39
Kr	30	96.3	111.2	35.19
Pr	0	98.2	98.2	64.64
Pr	45	68	96.1	92.01

6   Test Set-up and Procedures

SEE testing was performed on the SN55HVD233EVM-CVAL. The board was powered up using one (Channel # 3) of the four channels on an Agilent N6702A precision power supply. The current clamp was set to 500 mA (> 10 times nominal current). The SEE Events were monitored by using the Tektronix DPO7254C Digital Phosphor Oscilloscope (4-channel, 40 Gsps). The scope has a 3.2μs update rate under the conditions used when collecting data at TAMU (Fast-Frame). The update rate represents the amount of time to re-arm the scope trigger after an event.

The HVD233-SP was tested on *Dynamic* mode.

Dynamic testing was conducted with a square wave signal driven into D with internal loopback disabled. (LBK = Low).

- Fast mode (500 kHz)
- Slow mode (50 kHz or 10 kHz)

For each test the receiver and the bus were monitored, the receiver was used as the trigger signal. On Dynamic Testing, the signal was provided by means of an Agilent 33220A AWG. The test signal used was a square wave with a 50% duty cycle and amplitude of 0 V–3.3 V driven onto. The bus was loaded with 60 Ω at all times. Pulse-Width (positive and negative) was used to capture the deviations of the expected output signal on the DPO7254C.

During SET testing, the current on the power supply was monitored at all times by means of a custom-developed LabVIEW™ Graphical User Interface (GUI) Radiation Test Program (PXI Rad-Test) running on a National Instruments NI-PXIe-8135 controller. The GUI provided control over the power source and recorded the beam start and stop output signal (5-V signal) on the TAMU system. The signal generators were controlled by means of the GPIB protocol using their respective drivers running on LabVIEW. The DPO7254C was controlled by its front-panel interface. The DPO was left in the cave at all times; however, a KVM extender was used to control it from upstairs (TAMU control room). For the testing, a positive and negative polarity pulse width trigger (±2% of the expected pulse width) was used. Figure 7 presents a block diagram of the setup used during the SEE testing and Table 3 presents the equipment setup. For the SEL testing, the device was heated using a convection heat gun aimed at the die. The junction temperature was monitored by using a K-Type thermocouple attached as close as possible to the die.

Table 3. Equipment Set Used for the SEE Testing

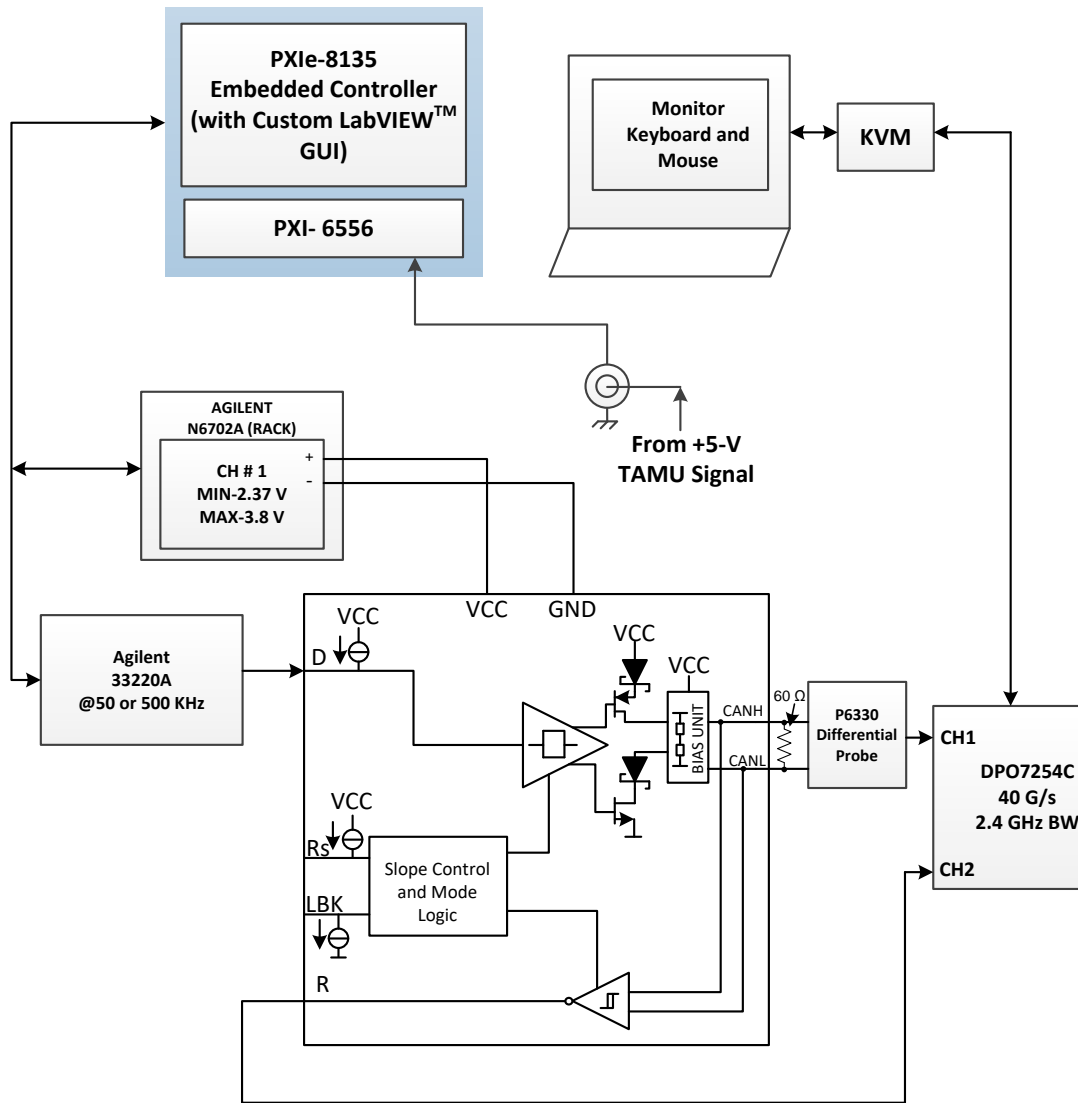| Pin Name	Equipment Used	Capability	Compliance	Range of Values Used
VCC-GND	Agilent N6702A (Channel #3)	5 A	500 mA	3 V and 3.3 V
D	Agilent 33220A	20 MHz	-	50 and 500 kHz
Digital Scope	DPO7254C	40 Gsps (2.4 GHz BW)	-	20 Gsps at 2.4 GHz BW

Figure 7. Block Diagram of Heavy-Ion SET Test Setup With the HVD233-SP

7   Results

7.1   *Single-Event Latch-Up (SEL)*

During SEL characterization, the device was heated using forced hot air, maintaining the die temperature at 125°C. The temperature was monitored by means of a K-type thermocouple attached as close as possible to the die. The species used for the SEL testing was a praseodymium (^{59}Pr) ion with an angle-of-incidence of 45° degrees for an LET_{EFF} = 92 MeV-cm^2/mg. The kinetic energy in the vacuum for this ion is 0.885 GeV (15 MeV/amu line). A flux of approximately 1.0×10^5 ions/cm^2-s and a fluence of approximately 1.0×10^7 ions were used for all seven runs. The VCC voltage was set to the recommended maximum at 3.6 V. Run duration to achieve this fluence was approximately 2 minutes. No SEL events were observed during all seven runs. The SEL tests were conducted in Dynamic Mode with the part clocked at 10 kHz, and static on a recessive mode as described in Table 4.

Figure 8 shows the plot of the current versus time and Figure 9 shows the temperature versus time for run # 1 (active at 10 kHz).

Table 4. HVD233-SP SEL Conditions Using ^{59}Pr at an Angle-of-Incidence of 45°

Run #	Dev #	Average Flux (MeV-cm^2/mg)	Conditions				
			LBK	D	Bus Load	Rs	Bus Common Mode Voltage (V)
1	1	1.05×10^5	High	10 kHz	60 Ω	Low	N/A
2	1	9.86×10^4	High	10 kHz	60 Ω	Low	N/A
3	1	9.66×10^4	High	H	60 Ω	Low	6
4	1	9.40×10^4	High	H	60 Ω	Low	6
5	1	1.05×10^5	High	H	60 Ω	Low	12
6	1	1.05×10^5	High	H	60 Ω	Low	14
7	1	9.96×10^4	High	H	60 Ω	Low	18

No SEL events were observed, indicating that the HVD233-SP is SEL-immune at LET_{EFF} = 92 MeV-cm^2/mg and T=125°C. Using the MFTF method described in Appendix B and combining (or summing) the fluences of the seven runs (7.0 x 10^7), the upper-bound cross section (using a 95% confidence level) is calculated as:

$$\sigma_{SEL} \leq 5.27 \times 10^{-8} \text{ cm}^2 \text{ for } LET_{EFF} = 92 \text{ MeV-cm}^2/\text{mg and } T = 125°C \tag{1}$$
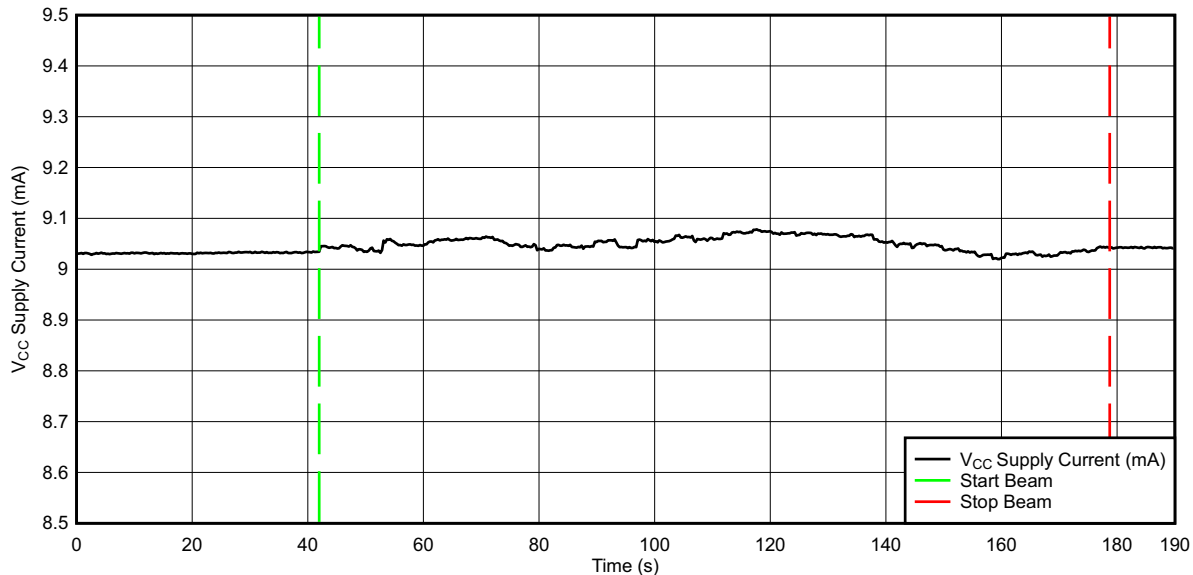

Figure 8. Current vs Time (I vs t) Data for VCC Supply Current During SEL Run # 1
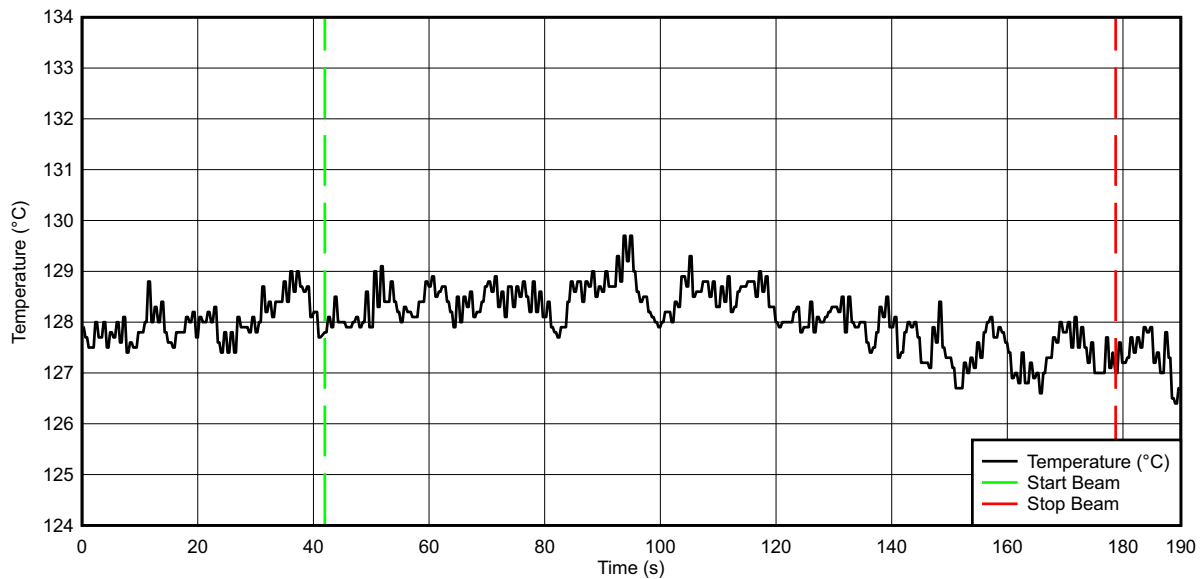
Figure 9. Temperature vs Time Data for SEL Run # 1

7.2 Single-Event Transient (SET)

The SET testing of the HVD233-SP was performed at room temperature using three units. Copper, Krypton, and Praseodymium heavy-ions were used for the characterization providing an LET_{EFF} ranging from 20 to 92 MeV-cm^2/mg (using angles). SET was characterized using dynamic conditions. As observed in Figure 7, the Bus and Receiver were monitored at all times, but the signal used for the trigger was the receiver. Most of the testing was conducted using fast mode (500 kHz) with the exception of run 32 at slow mode (50 kHz). The events were defined as a deviation of ±2% of the expected pulse width on the receiver. The bus was loaded with 60 Ω using a discrete resistor soldered on the evaluation module at all times. When monitoring the signals after a trigger, it was observed that not all events affect the driver and receiver circuits at the same time. For that reason, the data was categorized as driver and receiver events. As can be observed, a driver event will create an event on the receiver also (due to the bus loopback). To categorize the events as receiver or driver, the data was post-processed and the total number of driver events was subtracted from the total number of trigger events on the receiver to calculate the receiver events.

The summary of the dynamic testing is presented in Table 5. Cross section plots for the driver and receiver under dynamic testing is presented in Figure 10 and Figure 11. A Weibull fit is overlaid on each cross section plot and the parameters used are presented in Table 6. The equation used for the Weibull fit is presented in Equation 2. A histogram of the pulse-width deviation is presented for the driver and receiver in Figure 12 and Figure 13, respectively. Typical time domain plots for dynamic testing are presented in Figure 14 through Figure 17 for driver and receiver events (in each case, both signals are shown).

For the dynamic testing, positive and negative pulse-width triggers were used; however, all data was combined to calculate the cross section. The reason to do so is that events look very similar under the positive and negative polarity pulse-width trigger. To calculate the cross section for a specific LET_{EFF}, the total number of events and fluence were combined (summed). Using the MFTF method described in Appendix B, the upper bound cross section at 95% confidence interval was calculated.

7.2.1 Dynamic Testing

Table 5 details the HVD233-SP dynamic SET testing conditions.

Table 5. HVD233-SP Dynamic SET Testing Conditions[1]

Run #	Unit #	Ion	Angle	LET_{EFF} (MeV-cm²/mg)	Flux (ions·cm²/mg)	Fluence (# of ions)	Receiver Events	Bus Events
8	4	Cu	0	20	1.15×10^4	1.00×10^6	71	73
9	4	Cu	0	20	1.12×10^4	1.00×10^6	99	27
10	4	Kr	0	30	1.09×10^4	1.01×10^6	129	44
11	4	Kr	0	30	1.18×10^4	9.97×10^5	115	39
12	4	Kr	0	30	1.21×10^4	9.97×10^5	107	108
13	4	Kr	0	30	9.49×10^3	9.98×10^5	109	108
14	4	Kr	30	35	9.89×10^3	1.31×10^6	214	77
15	4	Kr	30	35	1.06×10^4	1.00×10^6	139	67
16	4	Kr	30	35	1.03×10^4	9.96×10^5	169	57
17	4	Kr	30	35	1.04×10^4	1.00×10^6	176	138
18	4	Kr	30	35	1.09×10^4	9.96×10^5	143	129
19	4	Kr	30	35	1.27×10^4	1.00×10^6	156	147
20	2	Pr	0	64	1.07×10^4	1.00×10^6	193	124
21	2	Pr	0	64	1.07×10^4	9.96×10^5	185	129
22	2	Pr	0	64	1.15×10^4	1.01×10^6	206	130
23	2	Pr	0	64	1.07×10^4	9.98×10^5	211	96
24	2	Pr	0	64	9.80×10^3	1.00×10^6	219	106
25	2	Pr	0	64	1.03×10^4	1.00×10^6	217	94
26	2	Pr	45	92	9.68×10^3	9.98×10^5	264	114
27	2	Pr	45	92	9.99×10^3	1.00×10^6	257	121
28	2	Pr	45	92	9.95×10^3	9.98×10^5	256	124
29	2	Pr	45	92	9.38×10^3	9.99×10^5	235	151
30	2	Pr	45	92	1.03×10^4	9.97×10^5	247	144
31	2	Pr	45	92	1.06×10^4	9.99×10^5	238	156
32	5	Pr	45	92	1.16×10^4	1.00×10^6	0	470

[1] For runs 8-32 the Rs pin was connected to GND and the frequency on the Driver was set to 500 kHz. The exemption to this was run # 32 in which Rs pin was connected via 50 kΩ to GND and the driver frequency was set to 50 kHz.

7.2.2   Cross Section for Dynamic Testing

Figure 10 and Figure 11 illustrate the cross section versus LET_{EFF} for driver and receiver events dynamic testing, respectively.
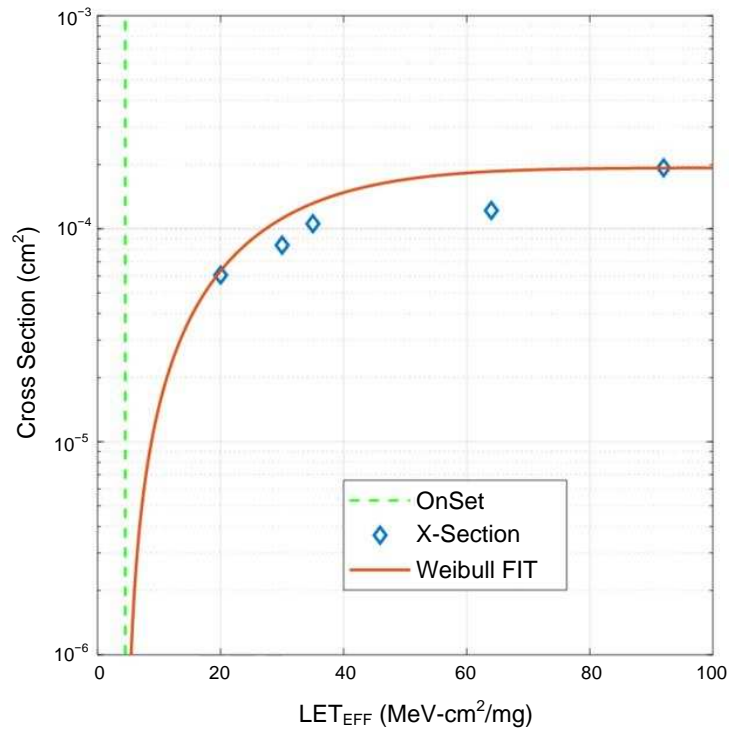

Figure 10. Cross Section vs LET_{EFF} for Driver Dynamic Testing
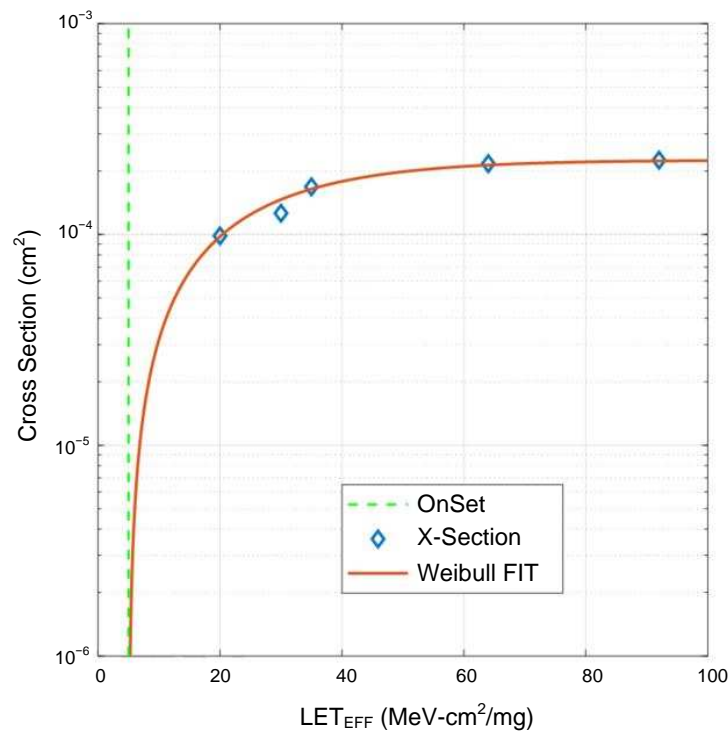
Figure 11. Cross Section vs LET$_{EFF}$ for Receiver Dynamic Testing

$$\sigma = \sigma_{SAT} \times \left(1 - e^{\left(-\frac{LET - Onset}{W}\right)^{s}}\right)$$

(2)

Table 6. Weibull Parameters for the Dynamic Testing

Parameter	Receiver Events Fit	Bus Events Fit
σ_{SAT}	2.28 x 10^{-4}	1.82 x 10^{-4}
Onset	5	4.5
W	24	28
s	1.2	1.56

7.2.2.1   *Pulse-Width Distribution Histogram for Dynamic Testing*
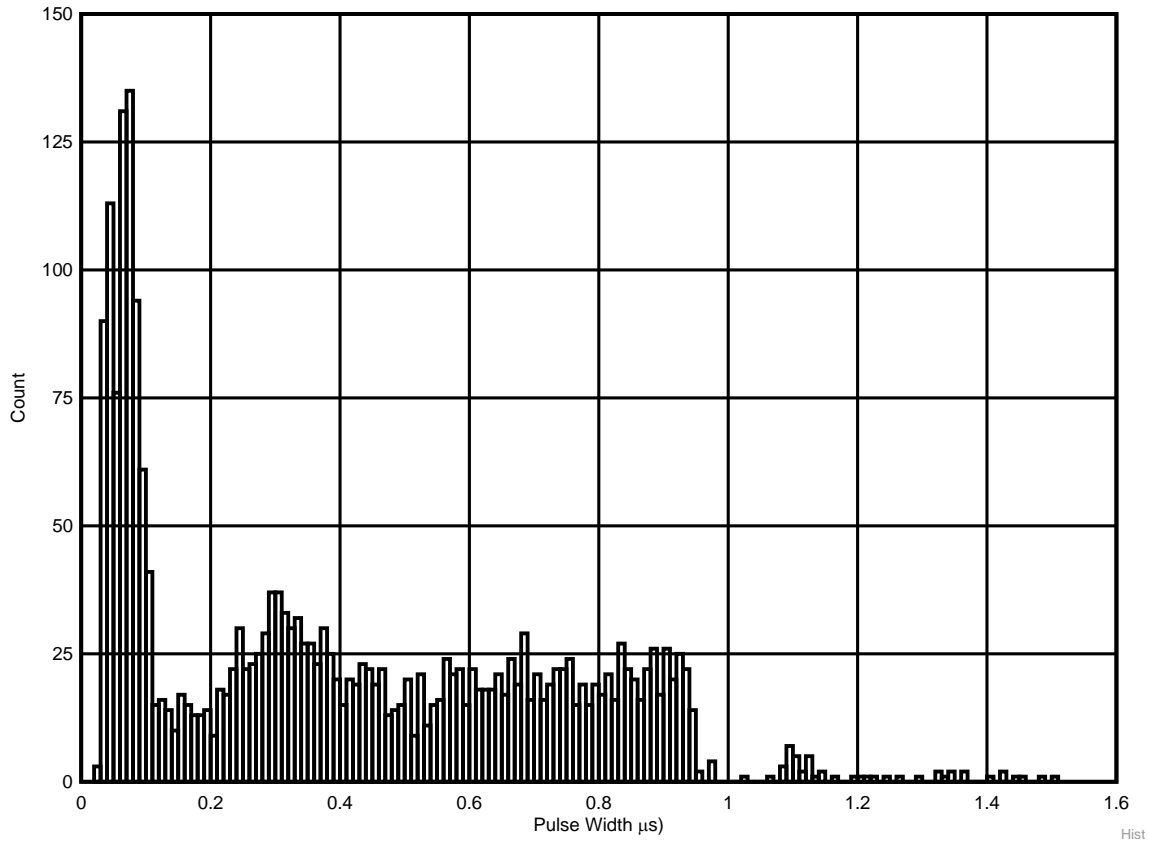
Figure 12. Histogram of Pulse Width Distribution on Driver Events (Dynamic at 500 kHz)
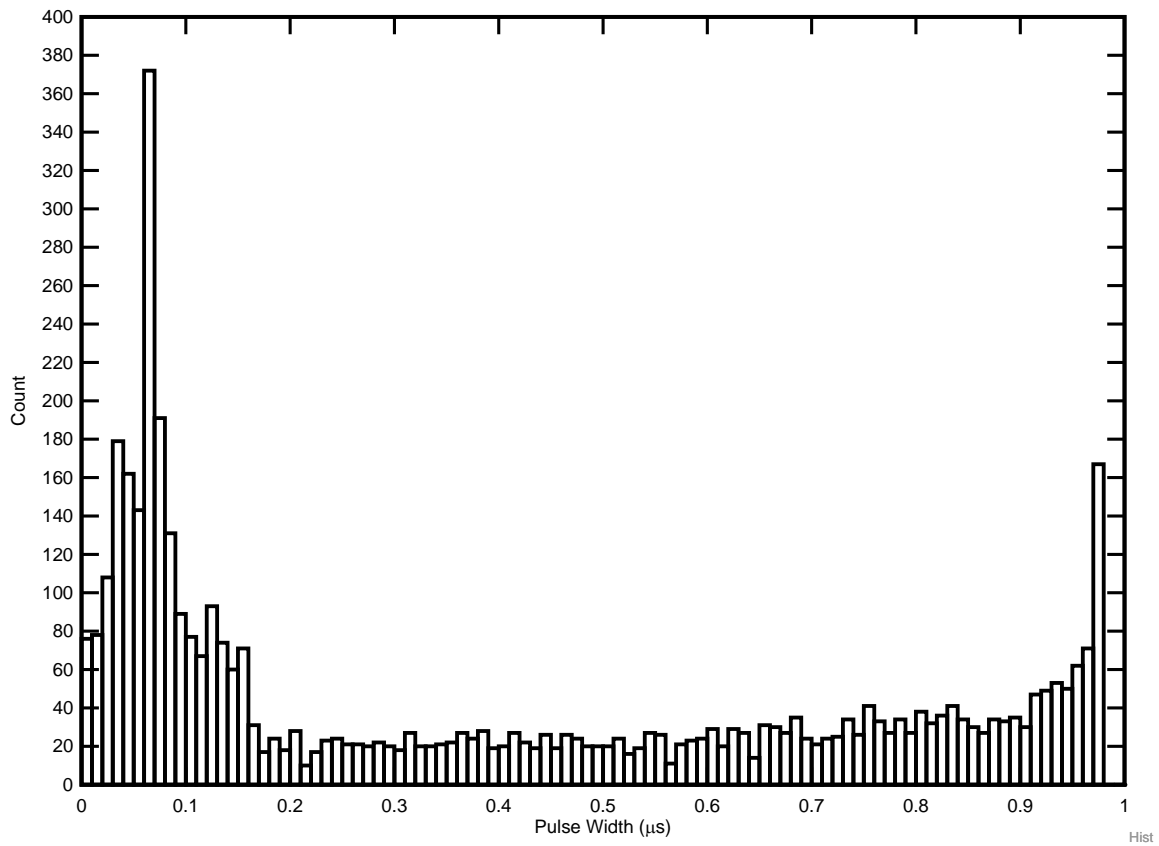
Figure 13. Histogram of Pulse Width Distribution on Receiver Events (Dynamic at 500 kHz)

NOTE: One event showed a pulse width of 3.15 µs, but it is not shown in this histogram for better appreciation of the distribution.

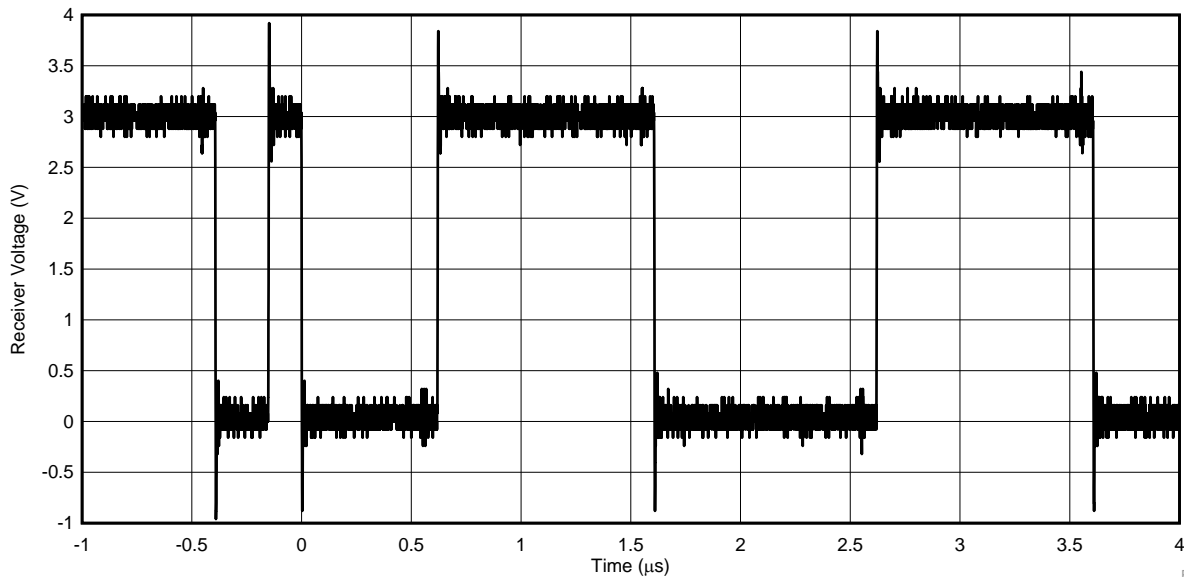### 7.2.2.2 *Time-Domain Plots for Dynamic Testing*

7.2.2.2.1 *Driver Event*
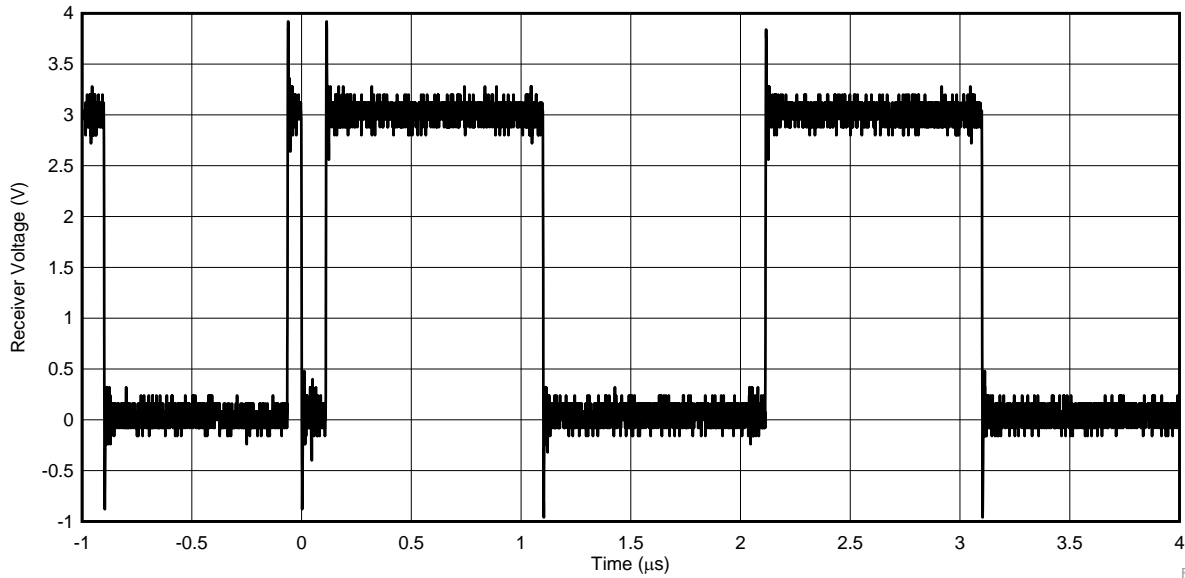
Figure 14. Time Domain Plot of the Receiver on Run # 26 (Event # 1)
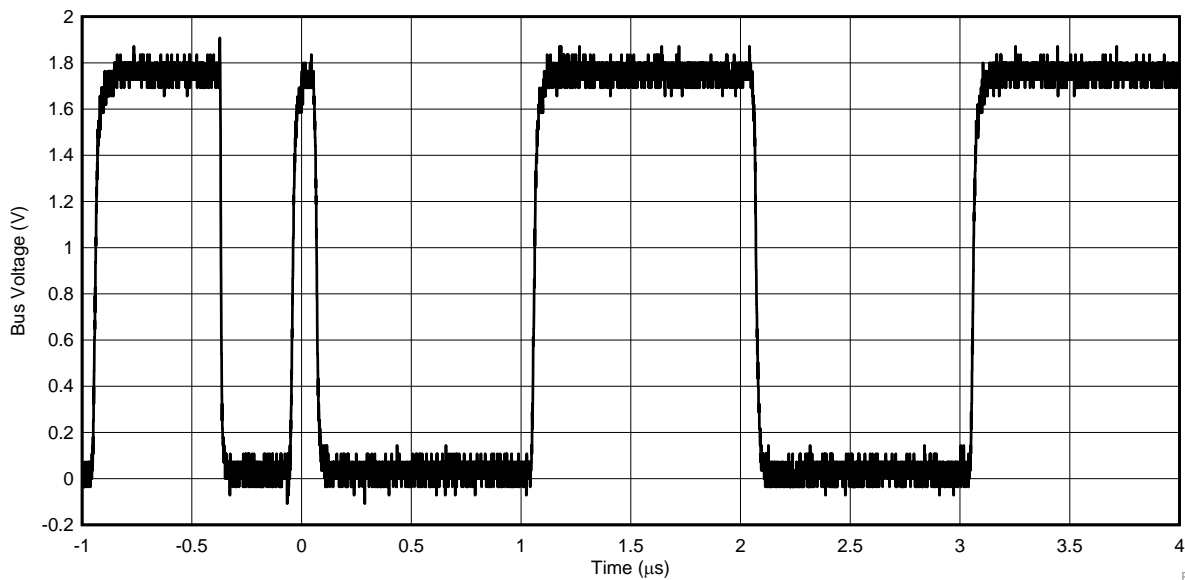
Figure 15. Time Domain Plot of the Bus on Run # 26 (Event # 1)

7.2.2.2.2 Receiver Event

Figure 16. Time Domain Plot of the Receiver on Run # 26 (Event # 277)
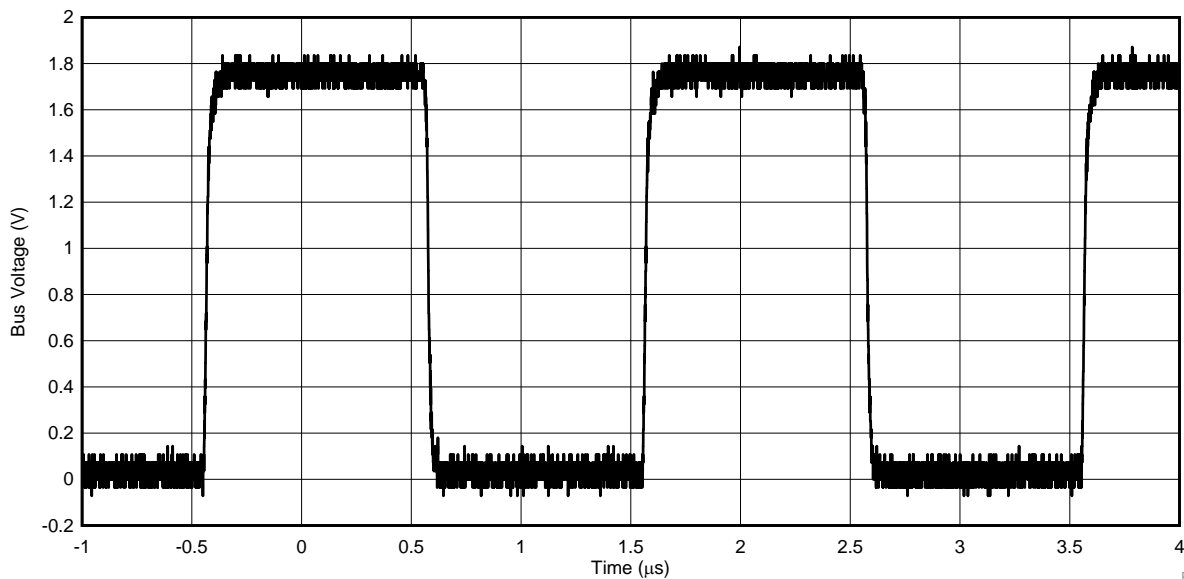
Figure 17. Time Domain Plot of the Bus on Run # 26 (Event # 277)

8   Event Rate Calculations

Event rates were calculated for LEO (ISS) and GEO environments by combining CREME96 orbital integral flux estimations and simplified SEE cross sections according to methods described in Appendix C. Assume a minimum shielding configuration of 100 mils (2.54 mm) of aluminum, and *worst-week* solar activity (this is similar to a 99% upper bound for the environment). Using the 95% upper-bounds for the SEL, SET (Driver), and SET (Receiver) the event-rates of the HVD233-SP are tabulated in Table 7, Table 8, and Table 9, respectively.

Table 7. SEL Event Rate Calculations for Worst-Week LEO and GEO Orbits

Orbit Type	Onset LET (MeV-cm²/mg)	CREME96 Integral Flux (/day·cm²)	σ SAT (cm²)	Event Rate (/day)	Event Rate (FIT)	MTBE (Years)
LEO (ISS)		8.18×10^{-7}		4.31×10^{-14}	1.80×10^{-6}	6.35×10^{10}
GEO	92.0	2.17×10^{-6}	5.27×10^{-8}	1.14×10^{-13}	4.77×10^{-6}	2.39×10^{10}

Table 8. SET (Driver) Event Rate Calculations for Worst-Week LEO and GEO Orbits

Orbit Type	Onset LET (MeV-cm²/mg)	CREME96 Integral Flux (/day·cm²)	σ SAT (cm²)	Event Rate (/day)	Event Rate (FIT)	MTBE (Years)
LEO (ISS)		1.64×10^{2}		2.98×10^{-2}	1.24×10^{6}	9.20×10^{-2}
GEO	4.5	1.49×10^{3}	1.82×10^{-4}	2.71×10^{-1}	1.13×10^{7}	1.01×10^{-2}

Table 9. SET (Receiver) Event Rate Calculations for Worst-Week LEO and GEO Orbits

Orbit Type	Onset LET (MeV-cm²/mg)	CREME96 Integral Flux (/day·cm²)	σ SAT (cm²)	Event Rate (/day)	Event Rate (FIT)	MTBE (Years)
LEO (ISS)		1.36×10^{2}		3.11×10^{-2}	1.30×10^{6}	8.81×10^{-2}
GEO	5.0	1.23×10^{3}	2.28×10^{-4}	2.79×10^{-1}	1.16×10^{7}	9.80×10^{-3}

MTBE is the mean-time-between-events in years at the given event rates. These rates clearly demonstrate the event rate of the HVD233-SP CAN Transceiver in two harshly conservative space environments. Customers using the HVD233-SP should only use the estimations provided in Table 7 through Table 9 as a rough guide and TI recommends that event rate calculations based on specific mission orbital and shielding parameters be performed to determine if the product will satisfy the reliability requirements for their specific mission. The onset used for this section was estimated using a Weibull fit, further testing will be conducted to determine the onset. The same is true for the static testing.

9 Summary

The purpose of this study was to characterize the effect of heavy-ion irradiation on the single-event effect (SEE) performance of the HVD233-SP CAN Transceiver. SEE experiments with heavy-ions having an LET_{EFF} ranging from 20–92 MeV-cm²/mg and fluences of 1.0×10^{6} to 1.0×10^{7} ions/cm² per run over minimum and maximum recommended voltage were conducted. The SEE results show the device is latch-up free up to 92 MeV-cm²/mg. The device was characterized under dynamic mode from 20–92 MeV-cm²/mg for transients and the cross-section plots with a Weibull fit are provided.

10 References

1. M. Shoga and D. Binder, "Theory of Single Event Latchup in Complementary Metal-Oxide Semiconductor Integrated Circuits", IEEE Trans. Nucl. Sci, Vol. 33(6), Dec. 1986, pp. 1714-1717.
2. G. Bruguier and J.M. Palau, "Single particle-induced latchup", IEEE Trans. Nucl. Sci, Vol. 43(2), Mar. 1996, pp. 522-532.
3. TAMU Radiation Effects Facility website. http://cyclotron.tamu.edu/ref/
4. "The Stopping and Range of Ions in Matter" (SRIM) software simulation tools website. http://www.srim.org/index.htm#SRIMMENU
5. D. Kececioglu, "Reliability and Life Testing Handbook", Vol. 1, PTR Prentice Hall, New Jersey,1993, pp. 186-193.
6. https://creme.isde.vanderbilt.edu/CREME-MC
7. A. J. Tylka, et al., "CREME96: A Revision of the Cosmic Ray Effects on Micro-Electronics Code", IEEE Trans. Nucl. Sci., 44(6), 1997, pp. 2150-2160.
8. A. J. Tylka, W. F. Dietrich, and P. R. Bobery, "Probability distributions of high-energy solar-heavy-ion fluxes from IMP-8: 1973-1996", IEEE Trans. on Nucl. Sci., 44(6), Dec. 1997, pp. 2140 – 2149.
9. A. J. Tylka, J. H. Adams, P. R. Boberg, et al.,"CREME96: A Revision of the Cosmic Ray Effects on Micro-Electronics Code", Trans. on Nucl. Sci, 44(6), Dec. 1997, pp. 2150 – 2160.

Total Ionizing Dose from SEE Experiments

The production HVD233-SP CAN Transceiver is rated for operation to a total ionizing dose (TID) of 50 krad(Si). In the course of the SEE testing, the heavy-ion exposures delivered a little bit less than approximately 1 krad(Si) per 1.0×10^6 ions/cm^2 run. The cumulative TID exposure for each device respectively, over all runs they each underwent, was determined to be 106 krad(Si) for device#1, 32.4 krad(Si) for device #2, 5.7 krad(Si) for device #3 and 0.9 krad(Si) for device # 4.

Confidence Interval Calculations

For conventional products where hundreds of failures are seen during a single exposure, one can determine the average failure rate of parts being tested in a heavy-ion beam as a function of fluence with a high degree of certainty and a reasonably tight standard deviation, and thus have a good deal of confidence that the calculated cross section is accurate.

With radiation-hardened parts however, determining the cross section becomes more difficult since often few, or even, no failures are observed during an entire exposure. Determining the cross section using an average failure rate with standard deviation is no longer a viable option, and the common practice of assuming a single error occurred at the conclusion of a null-result can end up in a greatly underestimated cross section.

In cases where observed failures are rare or non-existent, the use of confidence intervals and the chi-squared distribution is indicated. The chi-squared distribution is particularly well-suited for the determination of a reliability level when the failures occur at a constant rate. In the case of SEE testing, where the ion events are random in time and position within the irradiation area, one expects a failure rate that is independent of time (presuming that parametric shifts induced by the total ionizing dose do not affect the failure rate), and thus the use of chi-squared statistical techniques is valid (since events are rare, an exponential or Poisson distribution is usually used).

In a typical SEE experiment, the device-under-test (DUT) is exposed to a known, fixed fluence (ions/cm^2) while the DUT is monitored for failures. This is analogous to fixed-time reliability testing and, more specifically, time-terminated testing, where the reliability test is terminated after a fixed amount of time whether or not a failure has occurred (in the case of SEE tests fluence is substituted for time and hence it is a fixed fluence test)[5]. Calculating a confidence interval specifically provides a range of values which is likely to contain the parameter of interest (the actual number of failures per fluence). Confidence intervals are constructed at a specific confidence level. For example, a 95% confidence level implies that if a given number of units were sampled numerous times and a confidence interval estimated for each test, the resulting set of confidence intervals would bracket the true population parameter in about 95% of the cases.

To estimate the cross section from a null-result (no fails observed for a given fluence) with a confidence interval, we start with the standard reliability determination of lower-bound (minimum) mean-time-to-failure for fixed-time testing (an exponential distribution is assumed):

$$\text{MTTF} = \frac{2nT}{X^2_{2(d+1);100\left(1-\frac{a}{2}\right)}}$$

where

- MTTF = minimum (lower-bound) mean-time-to-failure
- n = number of units tested (presuming each unit is tested under identical conditions)
- χ^2 = the chi-square distribution evaluated at $100(1 - \alpha/2)$ confidence level
- d = the degrees-of-freedom (the number of failures observed)   (3)

With slight modification for our purposes, invert the inequality and substitute F (fluence) in the place of *T*:

$$MFTF = \frac{2nF}{X^2_{2(d+1);100\left(1-\frac{a}{2}\right)}}$$

where

- MFTF = mean-fluence-to-failure
- F = the test fluence
- χ^2 = the chi-square distribution evaluated at $100(1 - \alpha/2)$ confidence level
- d = the degrees-of-freedom (the number of failures observed)   (4)

The inverse relation between MTTF and failure rate is mirrored with the MFTF. Thus the upper-bound cross section is obtained by inverting the MFTF:

$$\sigma = \frac{X^2_{2(d+1);100\left(1-\frac{a}{2}\right)}}{2nF}$$

(5)

Assume that all tests are terminated at a total fluence of 1.0×10^6 ions/cm^2. Also assume there are a number of devices with very different performances that are tested under identical conditions. Assume a 95% confidence level ($\alpha = 0.05$). Note that as d increases from 0 events to 100 events the actual confidence interval becomes smaller, indicating that the range of values of the true value of the population parameter (in this case the cross section) is approaching the mean value + 1 standard deviation. This makes sense when one considers that as more events are observed the statistics are improved such that uncertainty in the actual device performance is reduced.

Table 10. Experimental Example Calculation [1]

degrees-of-freedom (d)	2(d+1)	χ^2 at 95%	Calculated Cross Section (cm^2)		
			Upper-Bound at 95% Confidence	Mean	Average + Standard Deviation
0	2	7.38	3.69×10^{-6}	0.00×10^0	0.00×10^0
1	4	11.14	5.57×10^{-6}	1.00×10^{-6}	2.00×10^{-6}
2	6	14.45	7.22×10^{-6}	2.00×10^{-6}	3.41×10^{-6}
3	8	17.53	8.77×10^{-6}	3.00×10^{-6}	4.73×10^{-6}
4	10	20.48	1.02×10^{-5}	4.00×10^{-6}	6.00×10^{-6}
5	12	23.34	1.17×10^{-5}	5.00×10^{-6}	7.24×10^{-6}
10	22	36.78	1.84×10^{-5}	1.00×10^{-5}	1.32×10^{-5}
50	102	131.84	6.59×10^{-5}	5.00×10^{-5}	5.71×10^{-5}
100	202	243.25	1.22×10^{-4}	1.00×10^{-4}	1.10×10^{-4}

[1] Experimental example calculation of MFTF and σ using a 95% confidence interval for several different observed results (d = 0, 1, 2,…100 observed events during fixed-fluence tests) assuming 1.0×10^6 ions/cm^2 for each test. Note that as the number of observed events increases the confidence interval approaches the mean.

Orbital Environment Estimations

To calculate on-orbit SEE event rates one needs both the device SEE cross section and the flux of particles encountered in a particular orbit. Device SEE cross sections are usually determined experimentally while flux of particles in orbit is calculated using various codes. For the purpose of generating some event rates, a Low-Earth Orbit (LEO) and a Geostationary-Earth Orbit (GEO) were calculated using CREME96. CREME96 code, short for Cosmic Ray Effects on Micro-Electronics is a suite of programs[6][7] that enable estimation of the radiation environment in near-Earth orbits. CREME96 is one several tools available in the aerospace industry to provide accurate space environment calculations. Over the years since its introduction, the CREME models have been compared with on-orbit data and demonstrated their accuracy. In particular, CREME96 incorporates realistic "worst-case" solar particle event models, where fluxes can increase by several orders-of-magnitude over short periods of time.

For the purposes of generating conservative event rates, the worst-week model (based on the biggest solar event lasting a week in the last 45 years) was selected, which has been equated to a 99%-confidence level worst-case event[8][9]. The integrated flux includes protons to heavy ions from solar and galactic sources. A minimal shielding configuration is assumed at 100 mils (2.54 mm) of aluminum. Two orbital environments were estimated, that of the International Space Station (ISS) which is LEO and the GEO environment. Figure 18 shows the integrated flux (from high LET to low) for these two environments.
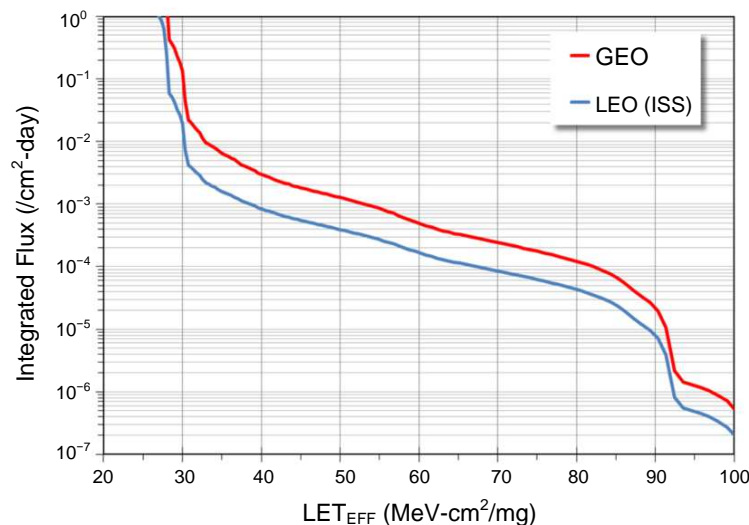
Integral particle flux vs LET_{EFF} for a LEO-ISS (blue curve) and a GEO (red curve) environment as calculated by CREME96 assuming worst-week and 100 mils (2.54 mm) of aluminum shielding. Note that the y-axis represents flux integrated from higher LET to lower LET. The value of integral flux at any specific LET value is actually the integral of all ion events at that specific LET value to all higher LETs.

Figure 18. Integral Particle Flux vs LET_{EFF}

Using this data, we can extract integral particle fluxes for any arbitrary LET of interest. To simplify the calculation of event rates we assume that all cross-section curves are square – meaning that below the onset LET the cross section is identically zero while above the onset LET the cross section is uniformly equal to the saturation cross section. Figure 19 illustrates the approximation, with the green curve being the actual Weibull fit to the data with the "square" approximation shown as the red-dashed line. This

allows us to calculate event rates with a single multiplication, the event rate becoming simply the product of the integral flux at the onset LET, and the saturation cross section. Obviously this leads to an over-estimation of the event rate since the area under the square approximation is larger than the actual cross-section curve – but for the purposes of calculating upper-bound event rate estimates, this modification avoids the need to do the integral over the flux and cross-section curves.
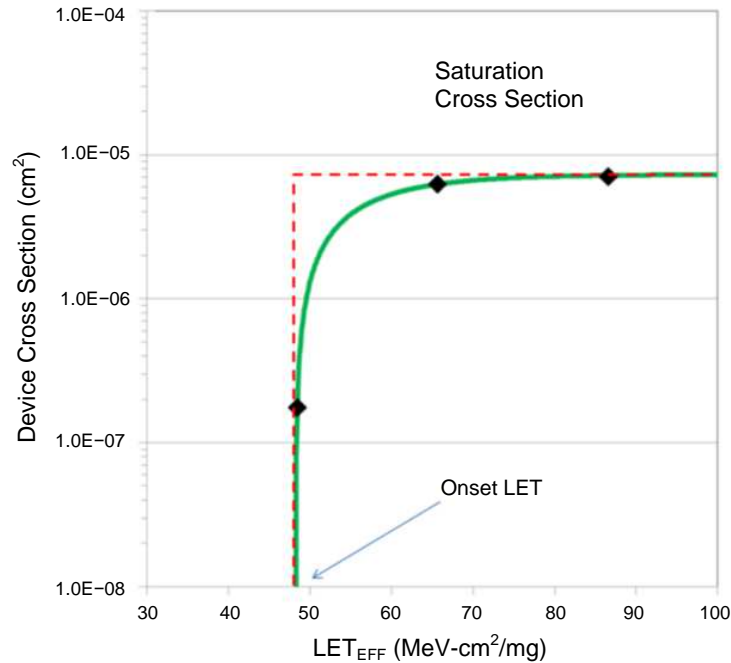
Device cross section vs. LET_{EFF} showing how the Weibull fit (green) is "simplified" with the use a square approximation (red dashed line)

Figure 19. Device Cross Section vs. LET_{EFF}

To demonstrate how the event rates in this report were calculated, assume that we wish to calculate an event rate for a GEO orbit for the device whose cross section is shown in Figure 19. Using the red curve in Figure 19 and the onset LET value obtained from Figure 18 (approximately 47 MeV-cm^2/mg) we find the GEO integral flux to be approximately 1.6×10^{-3} ions/cm^2-day. The event rate is the product of the integral flux and the saturation cross section in Figure 19 (approximately 7.5×10^{-6} cm^2):

$$GEO \;\; Event \;\; Rate = \left(1.6 \times 10^{-3} \frac{ions}{cm^2 \times day}\right) \times \left(7.5 \times 10^{-6} \;\; cm^2\right) = 1.2 \times 10^{-8} \frac{events}{day}$$

$$GEO \;\; Event \;\; Rate = 5.0 \times 10^{-6} \frac{events}{hr} = 0.5 \;\; FIT$$

$$MTBE = 234,000 \;\; Years$$

(6)